Sensors and Actuators B 236 (2016) 732–740

Contents lists available at ScienceDirect

Sensors and Actuators B: Chemical

journal homepage: www.elsevier.com/locate/snb

Development and validation of a seizure initiated drug delivery system for the treatment of epilepsy

Rikky Muller[b,e], Zhilian Yue[a], Sara Ahmadi[a], Winston Ng[b], Willo M. Grosse[a], Mark J. Cook[a,c,d], Gordon G. Wallace[a,*], Simon E. Moulton[a,*,1]

[a] ARC Centre of Excellence for Electromaterials Science, AIIM Facility, Innovation Campus, University of Wollongong, Wollongong, New South Wales 2522, Australia
[b] Department of Electrical and Electronic Engineering, University of Melbourne, Melbourne, Victoria, 3001, Australia
[c] Centre for Clinical Neurosciences and Neurological Research, St. Vincent's Hospital Melbourne, P.O. Box 2900, Fitzroy, Victoria 3065, Australia
[d] Department of Medicine, University of Melbourne, St. Vincent's Hospital, 35 Victoria Parade, Fitzroy, Victoria 3065, Australia
[e] Department of Electrical Engineering and Computer Science, University of California, Berkeley, CA 94720 USA

ARTICLE INFO

Article history:
Received 13 January 2016
Received in revised form 5 May 2016
Accepted 6 June 2016
Available online 7 June 2016

Keywords:
Epilepsy
Detection
Electronics
Polymer
Drug delivery

ABSTRACT

Delivery of small dosages of anti-epileptic drug (AED) directly into the brain from implantable degradable polymers has been reported to alleviate epilepsy activity in a GAERS animal model, however this system delivers a continuous dose of AED to the brain. We describe here the development of an active drug delivery system whereby AED delivery is initiated by the onset of an epileptic event and controlled by a custom hardware device. The system is comprised of an electrocortigographic (ECoG) data receiver, computational hardware, and a drug delivery component. The system initiates the release of an AED from an electrically conductive polymer when a seizure biomarker is detected above a pre-set threshold. Evaluation of the system showed that it is possible to vary the quantity of drug released linearly by varing the amount of charge injected into the drug loaded electroactive polymer. In addition it is possible to induce drug release within 10 s of injecting the charge, highlighting the responsive nature of the system. This work demonstrates a significant advance in the development of a device that combines the electronics capable of monitoring ECoG activity, detecting epileptic seizures and initiating drug delivery.

1. Introduction

Epilepsy is a chronic neurological condition characterized by recurrent seizures. The incidence of epilepsy in most developed countries is between 50 and 100 cases per 100,000 population per year, although it is estimated that up to 5% of a population will experience non-febrile seizures at some point in life [1,2]. Patients with medically intractable epilepsy have impaired ability to work or function socially [3]. Treatment with available anti-epileptic drugs (AEDs) provides adequate control in only 33% of patients (1,2). Neurostimulation based therapies have also been shown to reduce seizure activity, with typical reductions in seizure frequency of approximately 40% acutely and up to 50–69% after several years [4]. Surgical resection of the seizure focus can be performed in the case of focal seizures, however this procedure can only be applied to specific patients depending on the location of the focus [5]. The success rate of inducing long-lasting seizure remission from epilepsy surgery ranges from 25% for patients exhibiting extrahippocampal seizures origin to 70% in appropriately selected candidates [5].

There have been several potential mechanisms proposed as the basis of drug resistance in epilepsy, but there remains a great deal of uncertainty as to the precise cause [6,7]. Importantly, the side effects of those drugs prevent large increase in the dose [8]. Alternative therapies aimed at improving the availability of AEDs such as the intracranial implantation of polymer-based drug delivery systems are being investigated [9,10]. This targeted drug delivery approach has been shown to be useful in the treatment of animal models of several neurological disorders such as Parkinson's disease, Huntington's disease and Alzheimer's disease [11]. Also, Halliday et al. [10] used levetiracetam-loaded biodegradable polymer implants in the tetanus toxin model of temporal lobe epilepsy in rats; the results of this study indicated that drug-eluting poly-

* Corresponding authors.
E-mail addresses: gwallace@uow.edu.au (G.G. Wallace), smoulton@swin.edu.au (S.E. Moulton).
[1] Current address: Biomedical Engineering Faculty of Science, Engineering and Technology Swinburne University of Technology Hawthorn, Victoria, 3122, Australia.

http://dx.doi.org/10.1016/j.snb.2016.06.038
0925-4005/

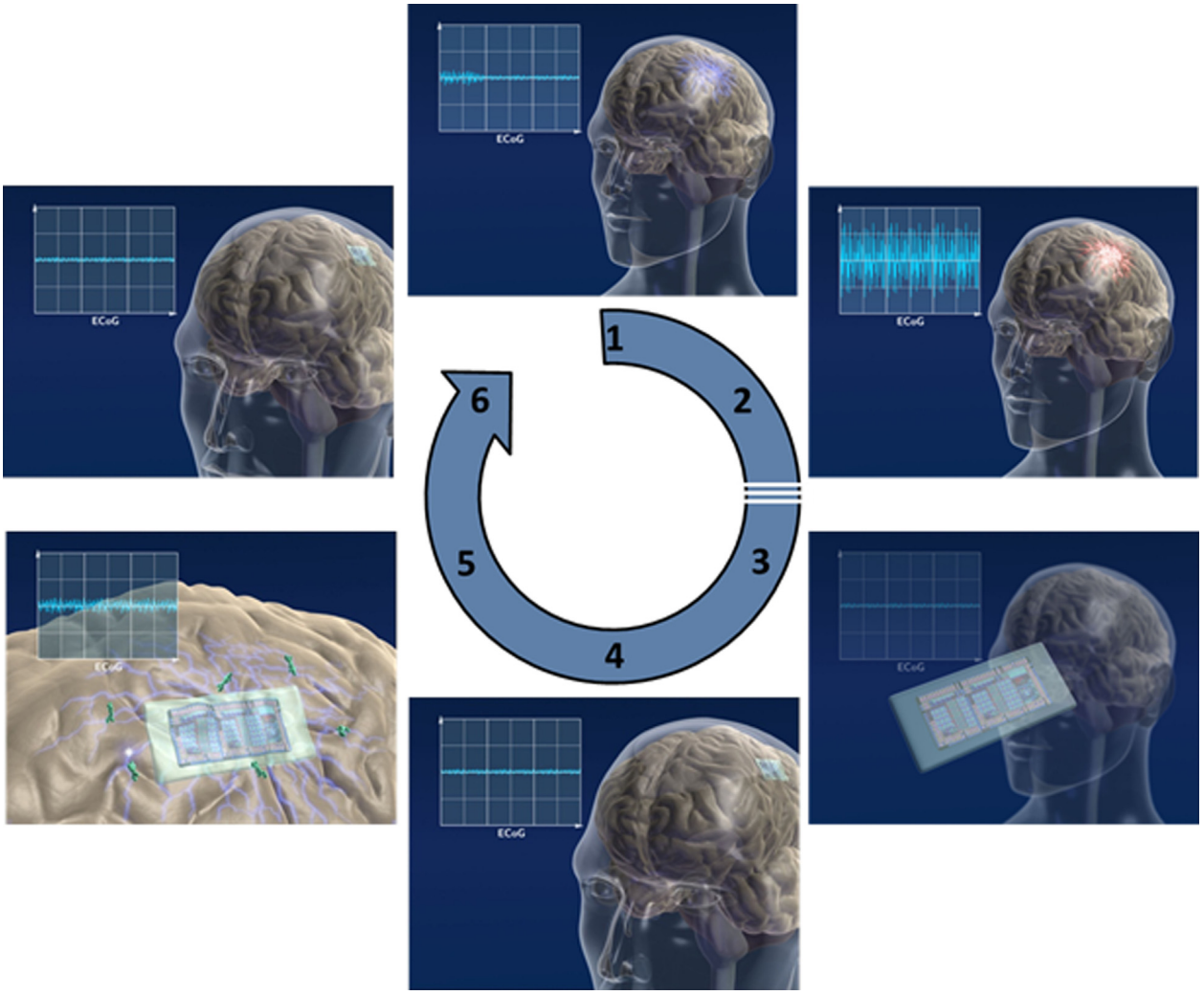

Fig. 1. Schematic of the seizure-initiated drug delivery system showing: (1) the onset of pre-seizures; (2) progression into an epileptic seizure event; (3 and 4) surgical intervention where by an AED loaded seizure detection and delivery device is implanted; (5) the implant detects the ECoG per-seizure and subsequently delivers the encapsulated AED (depicted as green molecules) and (6) due to the delivery of the AED at a therapeutic dosage the ECoG activity return to normal. The implant shown in part 3 is a stylized impression of the device and is not intended to represent the exact configuration of the system evaluated in this paper. (For interpretation of the references to colour in this figure legend, the reader is referred to the web version of this article.).

mer implants represent a promising evolving treatment option for intractable epilepsy.

Any system that relies on a reservoir of drug has a finite lifetime. Passive implantable drug delivery systems based on degradable polymers that continuously release drug [8], or discrete drug reservoirs with a finite number of doses [14], have very limited device lifetime due to rapid depletion of the reservoir. An intelligent, "on-demand" system, should possess the capability to identify a seizure through a specific biomarker and subsequently trigger drug release only when necessary. Such a system would increase the device lifetime by orders of magnitude when compared with passive implants. Salam et al. [12] describes an implantable detection and delivery device and highlights the release of a range of compounds to suppress epileptic activity. The system described in this paper utilizes a stimuli responsive polymer to deliver AED as opposed to a micropump used by Salma et al. In addition their latency time of approximately 16 s [12] is significantly slower than that reported here.

The schematic shown in Fig. 1 provides an illustrative concept of the system discussed in this paper. Sections 1 and 2 illustrate what occurs in patients with intractable epilepsy while sections 3 through to 6 illustrate how the system operates once implanted in patients. The system is comprised of electrodes and electronics capable of monitoring human ECoG signal and on detection of ECoG activity indicative of an epileptic seizure stimulate a conducting polymer doped with an AED. AED release is facilitated by an implantable microsystem that performs neural signal sensing and processing to detect the features of a seizure and to compute its onset, duration and intensity. The microsystem will then use these features to modulate the release of anti-epileptic drugs from the conducting polymers directly into the cortical tissue.

Polymer structures capable of triggering release in response to discrete thermal transitions [13,14], pH [15,16] or electrical stimuli [17–19] have some potential advantages in that release can be initiated in response to a change in environmental conditions or in response to an external electrical stimuli. Those based on the use of electrical stimulation have the advantage that the release profile can be tuned by the electrical stimulation parameters (current/potential magnitude and frequency) employed.

Conducting organic polymers represent a class of materials capable of responding to electrical stimulation to induce controlled release [20–22]. Release of incorporated molecules usually involves subjecting the polymer to an oxidation/reduction cycle. The efficiency of this process is determined by several factors such as

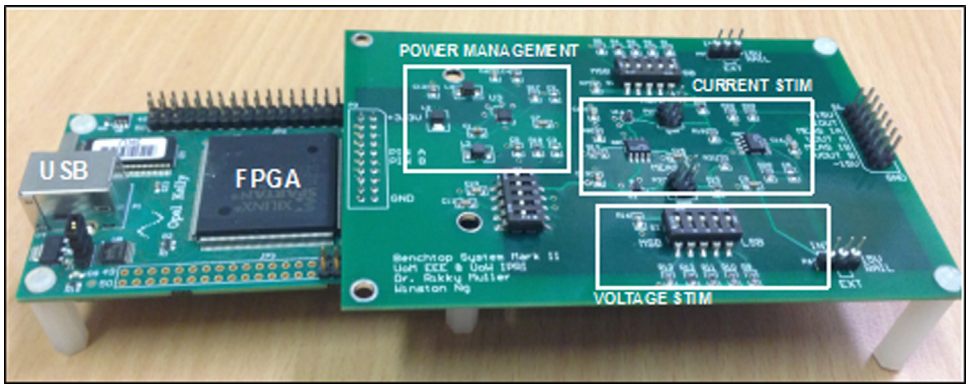

Fig. 2. Photo of the ECoG hardware system featuring a USB interface, a Xilinx field programmable gate array (FPGA), and custom-built current and voltage stimulators. Power management circuitry is designed to supply power to the stimulators.

polymer conductivity and the size of the incorporated molecule [23]. For example, anthraquinone disulphonic acid has been electrochemically released from a polypyrrole matrix [20], with the rate of release determined by the potential applied. The electrically stimulated release of the neurotrophin NT-3 from polypyrrole has also been reported [24]. The anti-inflammatory drug dexamethasone has been incorporated into polypyrrole (PPy) [18] or poly(3,4-ethylenedioxythiophene) (PEDOT) [22] and released using electrical stimulation.

This paper outlines the work conducted to develop an active controlled delivery system for the treatment of epilepsy that has the capability to deliver AEDs only at the time of a detected seizure event. In this study, we verify the system concept with custom prototyped hardware and by detecting the AED released from the PPy with an in-line UV–vis detector.

2. Materials and methods

The anti-epileptic drug fos-phenytoin (FOS) was a purchased from Sigmal-Aldrich and used as received. Pyrrole was purchased from Merck (Germany) and distilled prior to being used. The chemmicals used in prepararion of the artificial cerebrospinal fluid (aCSF) were purchased from Sigma Aldrich. The aCSF contained NaCl (0.866% w/v), KCl (0.224% w/v), $CaCl_2$-$2H_2O$; (0.0206% w/v) and $MgCl_2$-$6H_2O$ (0.0164% w/v) in 1 mM phosphate buffer (pH 7.4) (tablets from Sigma Aldrich), all prepared in Milli-Q water (18MΩ). UV–vis data was collected using quartz cuvettes (1.0 cm path length) obtained from Starna Pty Ltd. (Australia).

2.1. Polymer electrosynthesis and characterisation

FOS.phenytoin sodium salt (refered to as FOS) was incorporated into polypyrrole (PPy) as a dopant to give a PPy.FOS polymer film. The polymer was electrosynthesised galvanostatically at a current density of 0.5 mA cm^{-2} on gold-coated Mylar or gold coated quartz crystal microbalance (QCM) crystals from Milli-Q water containing 0.20 M pyrrole and 2.5 mM FOS. After deposition, the polymer coated electrode was rinsed thoroughly with deionised H_2O. The as-polymerized polymer coated electrode was dried in air for 48 h before use.

Electrochemical impedance spectroscopy (EIS) was carried out using a Gamry Impedance System, by subjecting coated electrodes to a 10 mV perturbation at a bias of 0 V. Cyclic voltammograms were obtained using the same three electrode electrochemical cell set-up as for synthesis, using EChem Software (version 2.0.14). Redox

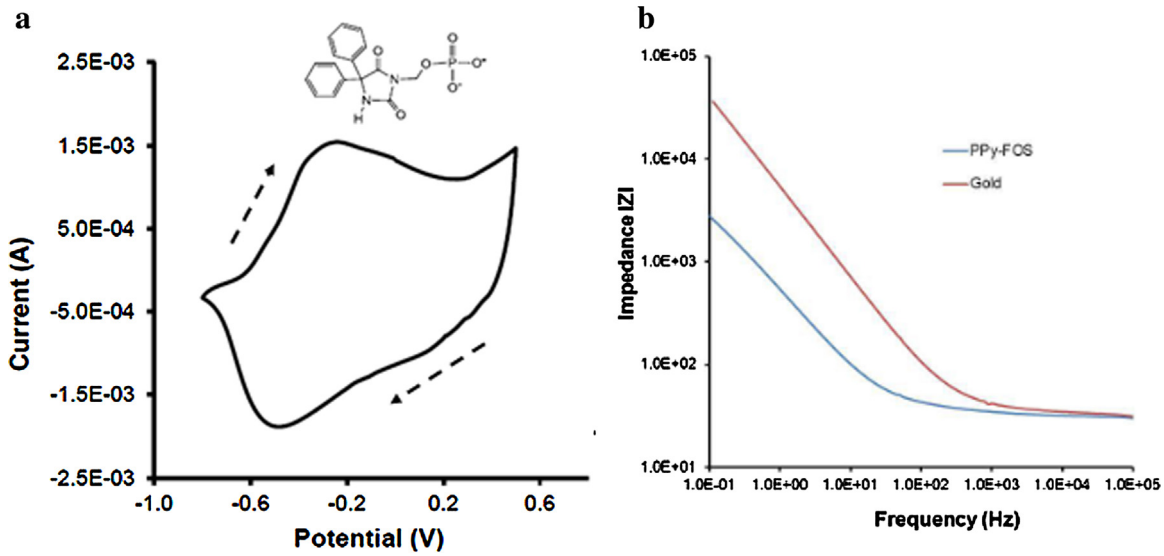

Fig. 3. Cyclic voltammogram (a) (CV) of PPy.FOS grown under optimized conditions of 2.5 mM FOS (chemical structure shown) and 0.5 mA/cm^2 current density for 2 min. The CV was recorded in aCSF at room temperature at a scan rate of 50 mV/s. The dashed arrows indicate the direction of the scanned potential. The electrochemical impedance spectroscopy (b) (EIS) recorded of the PPy.FOS (blue line) and gold coated Mylar (gold line). EIS was recorded at OCP in aCSF at room temperature utilizing an AC voltage of ±10 mV. (For interpretation of the references to colour in this figure legend, the reader is referred to the web version of this article.)

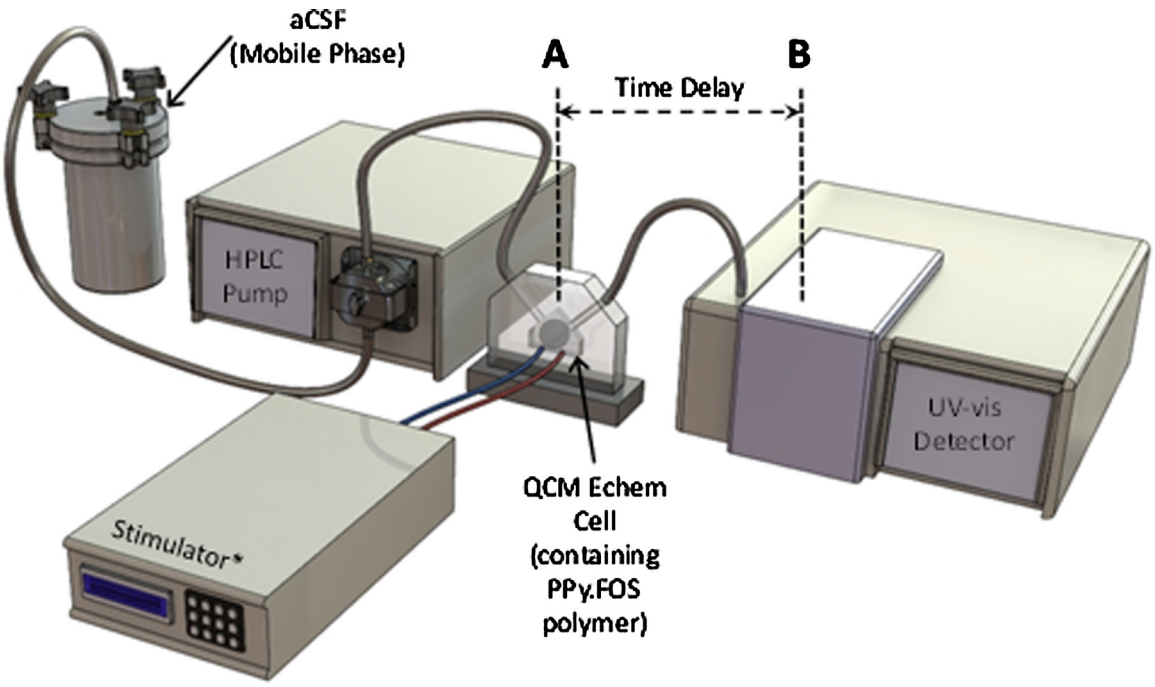

Fig. 4. Schematic of the system. The aCSF is pumped via the HPLC pump through the QCM Echem Cell and across the surface of the PPy.FOS coated QCM crystal (electrode) contained within. The aCSF (containing released drug) flows from the QCM Echem cell to the UV–vis detector then out to waste. A stimulator is connected to the QCM Echem cell in order to apply the stimulating voltage to the PPy.FOS coated QCM crystal (electrode). *The stimulator can either be the standard electrochemical equipment used to evaluate the system or the developed ECoG hardware electronics. The time between release at A and detection at B represents the delay time which is defined as the time it takes for the drug to travel from the PPy.FOS polymer to the UV–vis detector.

behaviour of the PPy.FOS coatings was examined over the potential window −0.8 V to ±0.5 V at a scan rate 50 mV/s.

2.2. FOS release from PPy.FOS polymers

The FOS release profiles from the PPy.FOS polymers was first evaluated using standard electrochemical equipment (an EDAQ e-corder®) to gain an understadning of the effects of electrical stimulation on release. The stimulated release was performed in a 3 electrode cell utilizing the PPy.FOS polymer as the working electrode, a platinum mesh auxilary electrode and a Ag/AgCl (3 M NaCl) reference electrode. Release was carried out in aCSF solution at room temperature. The release samples were analysed for FOS using UV–vis detection at 230 nm. The polymer was stimulated under passive, oxidizing and reducing conditions with each release condition being conducted in triplicate. The oxidation and reduction potentials were chosen from the cyclic voltamograms recorded from the PPy.FOS polymers.

2.3. Modified HPLC system for real time detection of FOS release

A modified HPLC system was developed to determine the amount of FOS released from the PPy.FOS polymers when stimulation was initiated using pre-recorded human ECoG data. The system consisted of a Shimadzu HPLC system with the column replaced by a Q-Sense QCM electrochemical (EChem) cell (Fig. 4) capable of housing the PPy.FOS polymer grown on the gold QCM crystal (using the optimal growth conditions described above for a total of 30 s). The QCM EChem cell is connected to either standard electrochemical equipment or the custom ECoG hardware system.

The ECoG hardware system is comprised of an Opal Kelly XEM3001 FPGA board comprised of a Xilinx Spartan 3 FPGA (Fig. 2). Xilinx ISE design software was used in the design and programming of the FPGA. Power management circuitry, voltage stimulator circuits and current stimulator circuits were designed with commercial off the shelf components and assembled on a custom printed circuit board. The USB data-streaming interface was programmed in MATLAB in conjunction with Opal Kelly software.

In order to quantify the amount of FOS released during electrical and ECoG stimulation a FOS calibration curve was established. The calibration curve was constructed using UV–vis data gathered from a serious of injections of FOS at various concentrations. The FOS injections were performed using the HPLC manual injection system without the use of the HPLC column as no column is used in the stimulated release experiments. The area under the UV–vis detection peak was plotted against the FOS concentration to obtain the calibration curve.

The system shown in Fig. 4 was validated using standard electrochemical equipment (EDAQ e-corder® potentiostat). In order to correlate stimulation conditions and subsequent drug release validation was performed using applied voltages. Drug release from PPy films is very well understood when voltages are used to stimulate release as demonstrated by the large number of publications detailing controlled release [24–25,26] Validation involved confirming that it was possible to apply a stimulating voltage to the PPy.FOS coated QCM crystal electrode and that the released drug could be detected in the UV–vis detector. In addition, the delay time (represented by the time it takes for the drug to flow from A to B in Fig. 4) was calculated at a range of aCSF flow rates. This delay time is critical as it provides the ability to calculate the time it takes for the drug to be released (at detectable amounts) after initiation of the electrical stimulation (termed “latency”) using Eq. (1).

$$latency = t_{total} - t_{delay} \quad (1)$$

Where t_{total} is the time between initiation of stimulation and the time of initial UV–vis detection, whilst t_{delay} is the time it takes for the aCSF containing the drug to travel from the QCM EChem cell (A – Fig. 4) to the UV–vis detector (B – Fig. 4). Initial UV–vis detection is taken to be when the UV–vis signal increases in excess of 5% above the baseline value. The UV–vis detector was set at 230 nm.

The value of t_{delay} was determined using a solution of toluidine blue (TB) as the mobile phase and measuring (visually) the time taken (t_1) for the TB solution to flow from the HPLC pump to the outlet of the QCM EChem cell. Using the same flow rate, the time (t_2) it takes for the TB solution to flow from the HPLC pump through the QCM Echem cell and to the UV–vis detector (UV–vis detector was set the wavelength of TB adsorption, namely 630 nm) was measured. Using Eq. (2) along with t_1 and t_2 values it is possible to calculate t_{delay}.

$$t_{delay} = t_2 - t_1 \quad (2)$$

3. Results and discusssion

3.1. Polymerisation and characterisation of polypyrrole doped with fos-phenytoin (PPy.FOS)

Optimization (data not presented) of the polymerisation conditions resulted in the ideal conditions for synthesis, being a FOS concentration of 2.5 mM and a current density of 0.5 mA/cm^2. Higher FOS concentrations resulted in non-uniform film formation whilst current densities above this resulted in excessive oxidation voltages being generated leading to over oxidised polymer.

Cyclic voltammetry using PPy.FOS as the working electrode shows a redox couple associated with the oxidation (−0.25 V) and reduction (−0.5 V) of the PPy.FOS polymer (Fig. 3a). The electrochemical impedance spectroscopy analysis of the PPy.FOS (Fig. 3b) shows a significant decrease in electrode impedance compared to the gold-coated Mylar upon which the polymer was grown. This decrease in impedance has been observed before [27] and is attributed to the increased surface area of the deposited polymer onto the gold coated Mylar. Low electrode impedance is central to enabling miniaturization of the proposed system since charge-based stimulation requires voltages that are proportional to the electrical impedance of the polymer.

3.2. Validation of in situ modified-HPLC FOS detection system

A schematic of the experimental set up to allow application of electrical stimulation and in-line, real time, detection of released FOS is shown in Fig. 4. Upon stimulation FOS was released from the polymer and flowed into the UV–visible detector. Using this set-up and injecting calibration standards (see experimental) the limit of detection was determined to be 25 ng and the linear dynamic range was 31 ng–20.3 μg.

An EDAQ e-corder electrochemical system was used to apply electrical stimulation to the PPy.FOS for 60 s with the current generated during stimulation recorded and used to calculate the charge passed (Fig. 5). Stimulation was only applied for 60 s, however from the traces in Fig. 5 the signal associated from the released drug lasts approximately 3–4 min. This is likely due to two factors, (i) the broadening of the drug dose as it travels through the tubing of the modified HPLC system from the QCM EChem cell to the UV–vis detector. This broadening results in the UV–vis data showing an increase in signal to a maximum and then a decrease as the FOS dose passes through the detector; and (ii) the time taken for the PPy.FOS to dissipate the charge accumulated during stimulation whereby release from PPy.FOS continues due to the charge on the polymer. Only very minor UV–vis detection peak broadening was observed during construction of the calibration curve (see experimental) suggesting that broadening observed in Fig. 5 is not associated with modified HPLC system artefacts and is most likely associated with the PPy.FOS properties. From Fig. 5 it is clear that there is a delay between applying stimulation and detecting drug release, this is termed latency and is associated with the PPy.FOS properties and can be separated out (see experimental section) from the time delay

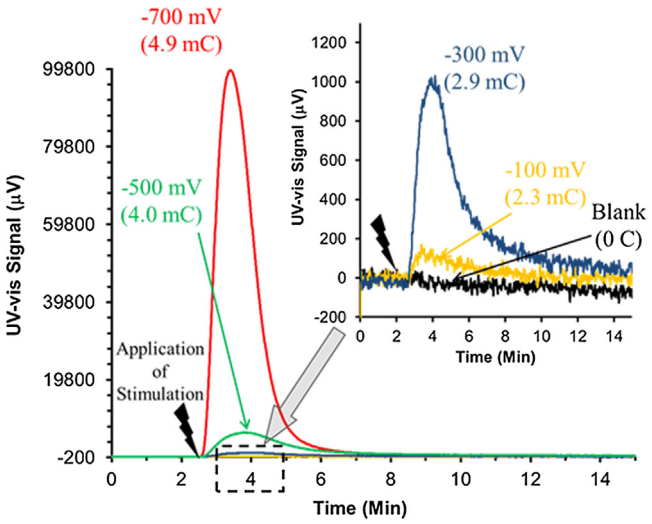

Fig. 5. UV–vis signal (μV) at 230 nm wavelength showing the effect of the applied potential and subsequent charge (Q) passed to the amount of FOS release through the detector. The listed voltages are the stimulation voltages used to initiate FOS release from the PPy.FOS polymer with charge (in brackets) calculated from the currents generated during stimulation. The time at which stimulation was applied is show with simulation lasting for 60 s. For clarity the release resulting from the lower magnitude stimulation voltages are shown in the inset.

inherent in the system shown in Fig. 3, and also discussed in the experimental section. The latency recorded from data in Fig. 5 is 10 ± 2 s.

The UV–vis data in Fig. 5 clearly shows variation in the detection signal as a function of the applied stimulation voltage. The current generated during voltage stimulation was recorded and converted to charge (Q) and is show in the brackets in Fig. 5. The area under the UV–vis signal is indicative of the amount of drug released from the PPy.FOS polymer, with the mass of drug calculated from the calibration curve. From Fig. 5 it is clear that the voltage applied (and charge injected) to the PPy.FOS polymer dramatically altered the amount of released drug. This result was also observed when positive potentials were applied to the polymer.

The mechanism for FOS release is proposed to involve electrostatic interactions as the application of electrical stimulation protocol increases the amount of FOS release compared to non-stimulation. From data presented in Figs. 5, 7 and 8 it is clear that as the amount of charge injected into the PPy.FOS increases so too does the extend of FOS release. However, both the ionic and hydrophobic properties of polypyrrole have been shown to vary upon application of electrical stimulus [28]. From the validation process it is clear that the system very efficiently detects the released FOS with minimal latency and that it is possible to study the effect of varying the stimulation conditions.

3.3. Detecting FOS release using pre-recorded human EEG signals

The EDAQ electrochemical system was replaced with a custom-built electronic hardware system pictured in (Fig. 2) and was connected to the flow QCM Echem cell (Fig. 4). The custom-built system is capable of detecting seizure onset from pre-recorded human intracranial EEG, or electrocorticography (ECoG), data recorded at 1kS/s. The data is streamed onto a commercial Field Programmable Gate Array (FPGA) from a computer and buffered to simulate real-time ECoG recording and digitization.

The ECoG system utilizes a custom algorithm that is implemented as digital hardware in the FPGA to compute the average line length of the recording, compare it to baseline, and trigger a seizure. Line length is a computationally efficient feature [29] that is

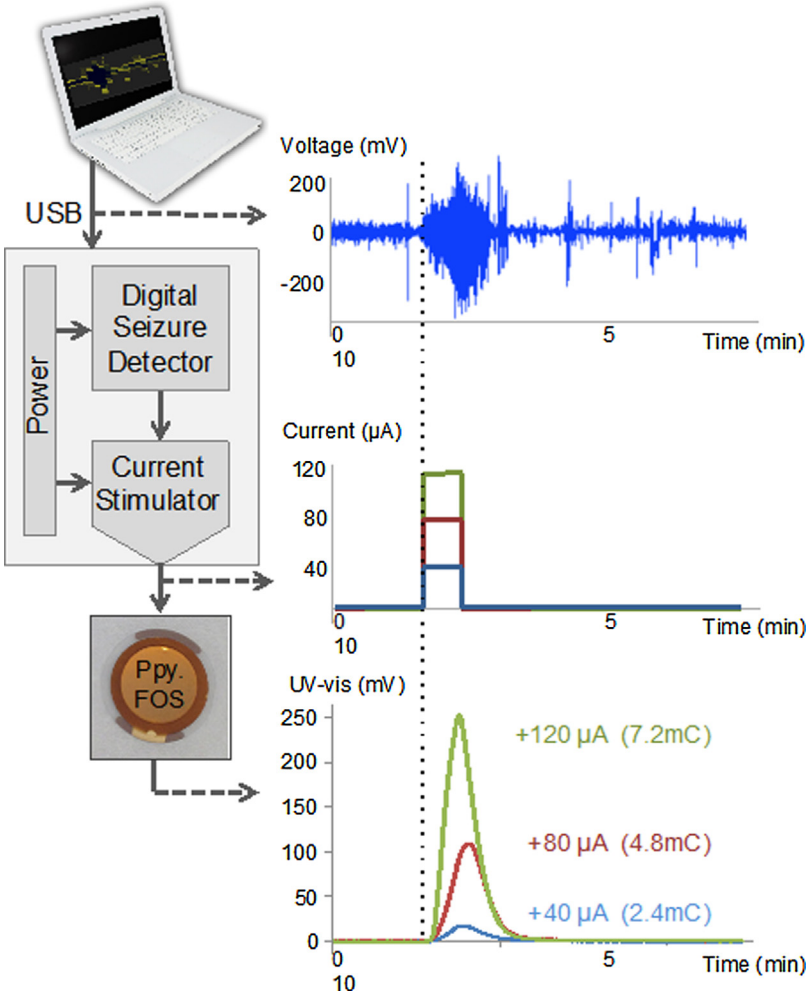

Fig. 6. Signal flow graph and corresponding interface signals of the ECoG system for three programmable output currents. The charge (Q) injected into the PPy.FOS during the applied current stimulation is shown in brackets.

extracted from human ECoG signals, which dramatically increases in magnitude during an epileptic seizure. When the line length of the recording window exceeds N times the baseline, where N is a pre-set threshold value greater than 1, the ECoG system is triggered to apply a programmable electrical stimulation pulse with a programmable duration to the PPy.FOS polymer to initiate FOS release as shown in Fig. 6. To reduce computational complexity, and therefore power, the ECoG system computes the line lengths every 0.1 s with a 1 s sliding window, thereby limiting the detection accuracy to less than 0.1 s. The trigger is coupled to the UV–vis detector for time-correlated readout of the two systems. In addition, a digital timer is employed on the hardware system to record detection timing. In this study, seizure detection thresholds were set manually by analysing the data offline. In future implementations, machine learning can be utilized to learn patient-specific and even electrode-specific thresholds.

The ECoG system utilizes custom stimulators that can be used in either current (0–1 mA) or voltage mode (0–1 V). Diverging from the voltage-stimulated validation of the system, the PPy.FOS polymers are stimulated using a constant current to provide more controlled release and limit the sample-to-sample variation. The use of applied currents is preferred in an *in vivo* environment as the use of voltages can result in uncontrolled and high currents being generated depending on the impedance of the *in vivo* environment [24,30], and therefore a high variation in the released quantity of drug. Using currents in this stage of the study permits us to evaluate the system under similar conditions as would be used for the intended application of *in vivo* drug delivery for the control of epilepsy.

Fig. 6 shows the signal flow of the hardware system with Fig. 7a and c show the resulting UV–vis data associated with FOS release initiated by the ECoG data through the hardware system. ECoG data is streamed via USB to the hardware platform and a digital seizure detector triggers stimulation current pulses with programmable amplitudes and pulse widths. The current pulses modulate the release of drug that is detected by the UV–vis detector. Multiple trials were conducted with a range of stimulation currents applied to the PPy.FOS polymer with 60 s pulse widths to quantify drug release and ascertain the versatility of the ECoG system and PPy.FOS combination. UV–vis data varies monotonically and is dependent on the magnitude of the applied current as well as the polarity of the current (Fig. 7a and c). The increase in UV–vis signal indicates that the amount of FOS release varies depending on the magnitude and polarity of the stimulating current (Fig. 7b and d). The latency (calculated from Fig. 7a and c) for the −80 and −120 μA data was calculated to be approximately 11 ± 2 s whilst for the lowest current tested (−40 μA) the latency increased slightly to 13 ± 3 s. This slight increase in latency is due to slow response of the PPy.FOS to this reduced current magnitude and indicates that higher applied currents are desirable to induce rapid drug release. At negative currents the time taken for the UV–vis trace to return to baseline after the maximum signal response (Fig. 7a) varied between

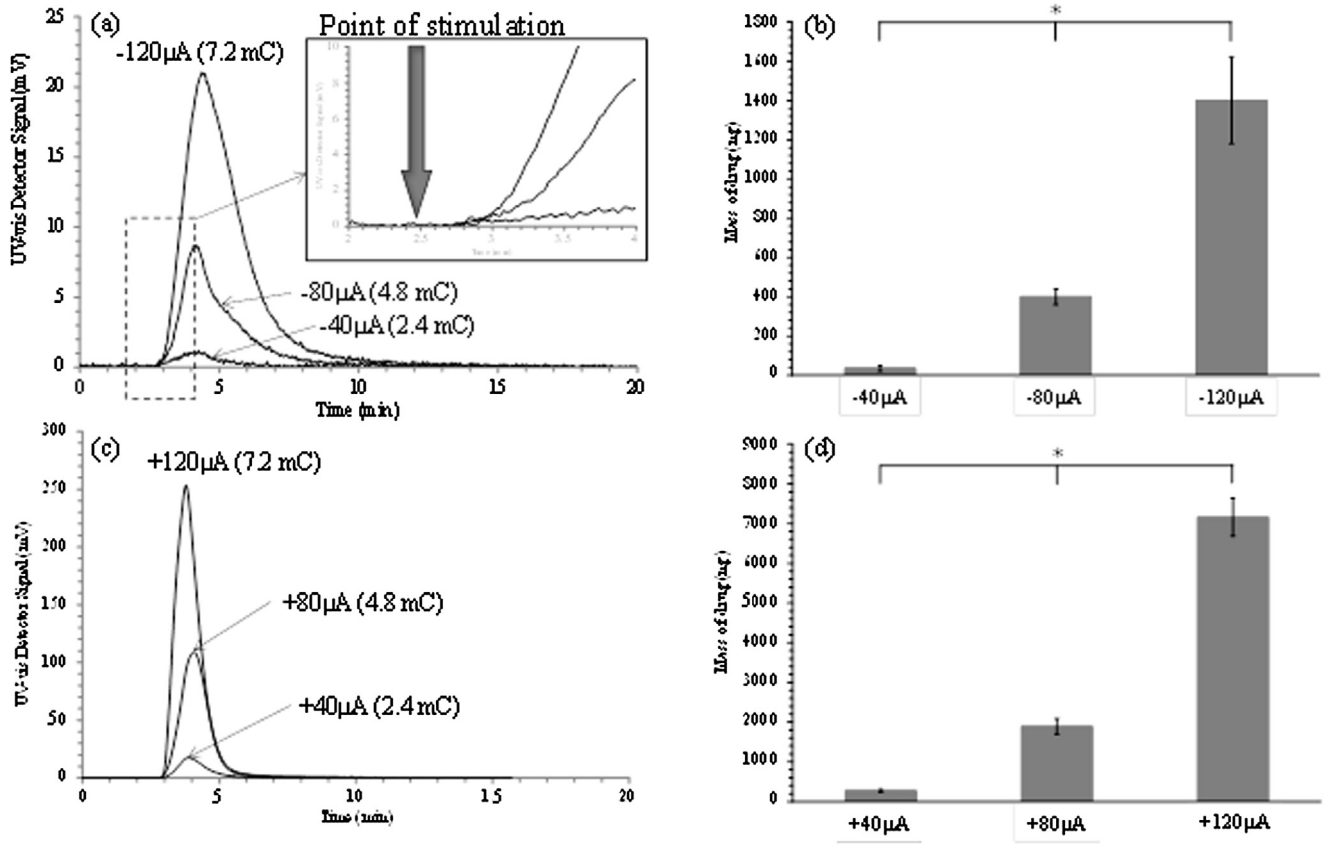

Fig. 7. UV–vis detection trace (a and c) generated when the ECoG stimulator stimulates the PPy.FOS for 60 s with a range of currents. The UV–vis detection is converted to mass of drug released (b and d) using the established calibration curve. The inset in (a) shows the point of applied stimulation (thick solid arrow) and appears at 2 min and 42 s. The errors represent the standard deviation about the mean ($p^* < 0.05$). The values in the bracket show the total charge injected during stimulation.

~2 min 30 s (−40 μA), ~7 min (−80 μA) and ~9 min (−120 μA). This time extension as the stimulating current increases is likely due to the increased drug release at higher currents resulting in a greater extent of FOS dose broadening in the systems tubing as well as the extended time taken for the PPy.FOS to dissipate the accumulated charge and return to the unstimulated state, thus resulting in drug release continuing after removal of the stimulation.

When the applied current polarity is positive the resulting UV–vis (Fig. 7c) and mass of drug (Fig. 7d) released is significantly higher compared to negative current stimulation (Fig. 7a and b). Under positive current stimulation the latency time was calculated to be approximately 10 ± 3 s, similar to the higher negative applied currents (Fig. 7a), however unlike the negative currents this latency time did not increase when the positive current value decreased to +40 μA. Whilst there appears to be a slight increase in the time it takes for the UV–vis trace to reach baseline at higher positive currents (Fig. 7c) the difference is only approximately 1 min (2 min 30 s for +40 μA compared to 3 min 30 s for +80 and +120 μA), which is much less than the time observed for the negative currents. Given that the extent of drug release under positive currents is significantly higher than for negative currents it would be expected that the time to return to baseline would be much larger if the effect of dose broadening within the systems tubing was a contributing factor (as suggested above). These results at positive current stimulation suggest that the time to reach baseline is governed by the time it takes for the PPy.FOS to dissipate the accumulated charge after the applied stimulation is removed. From these experiments it appears that this charge dissipation occurs faster when a positive current is used for stimulation. This result is significant since it is critical to cease drug release once stimulation is removed in order to avoid depletion of FOS from the PPy.FOS, and also to avoid unnecessarily high levels of the AED *in vivo*, which could lead to adverse patient side effects.

The data presented in Fig. 7 showed significant amounts of FOS being released when the currents were applied for 60 s. Given that the estimated amount of drug reaching the epileptic region of the brain under current systemic drug deliver treatment is 100–500 ng [31], these high level of FOS release are not necessary. Therefore the duration of the applied current was varied in order to study the effect on latency, PPy.FOS charge dissipation time and mass of FOS released, with the duration of stimulation varying between 15 s and 60 s at −120 μA and +120 μA (Fig. 8a and c respectively). Regardless of the stimulation time there was no observable change in the latency time with it remaining at the previously recorded 10 ± 2 s for +120 μA and 11 ± 2 s for −120 μA.

The time it takes for the UV–vis to reach baseline (PPy.FOS charge dissipation and hence cessation of FOS release) increases as the stimulation time increased. The relaxation time when −120 μA is applied for 15 s decreased to approximately 2 min 30 s compared to 7 min 30 s when stimulation was applied for 60 s (Fig. 8a). This increase is related to the amount of charge needed to dissipate once the stimulation is removed and the PPy.FOS returns back to it unstimulated state. The more charge generated during stimulation, either through longer stimulation times (at a constant current – Fig. 8) or higher currents (at a constant stimulation time – Fig. 7) the longer it takes for this charge to dissipate. As long as the PPy.FOS contains excess charge then the drug release phenomenon will continue. This excess charge could instantly be removed if the ECoG electronics system was able to apply a short circuit event to the

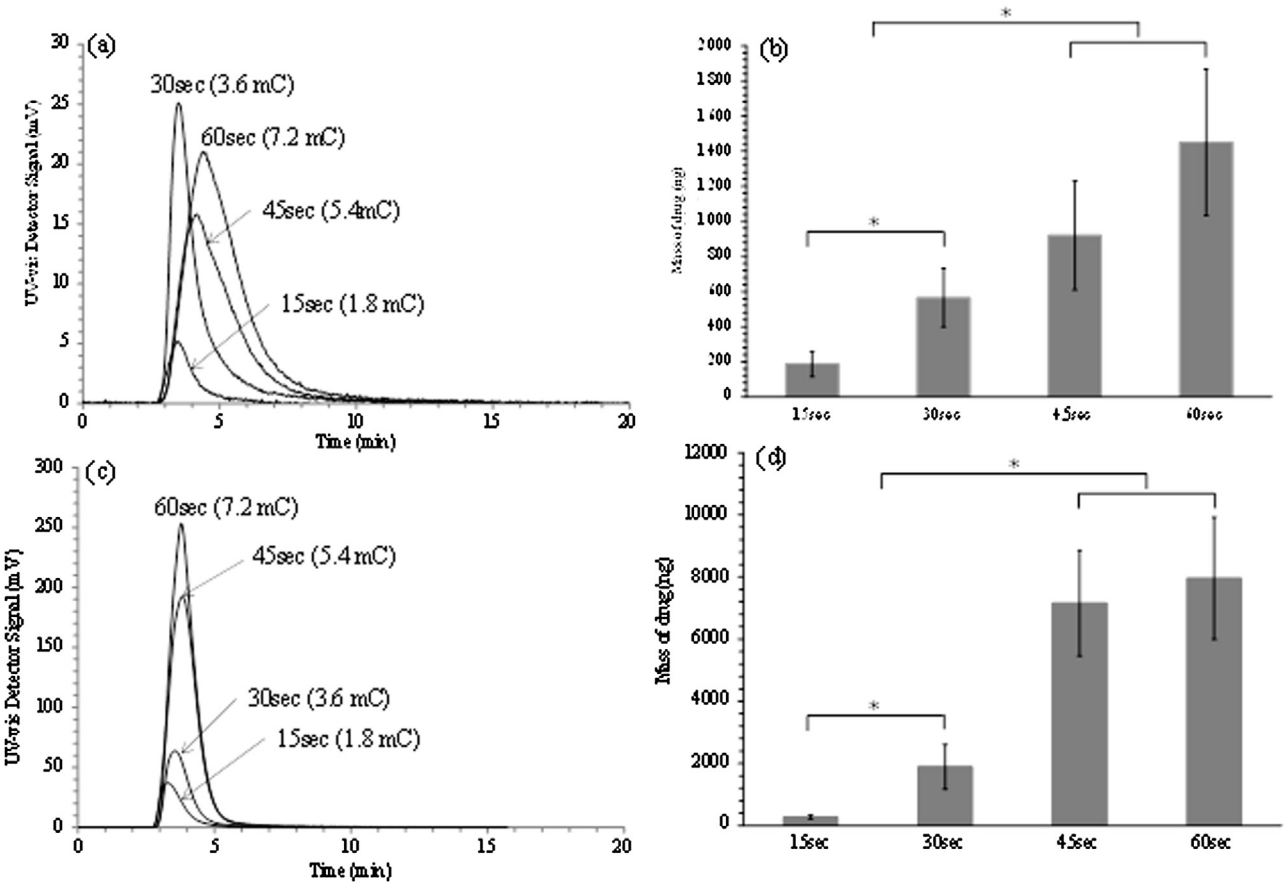

Fig. 8. UV–vis detection trace generated when the ECoG stimulator stimulates the PPy.FOS at −120 μA (a) and +120 μA (c) for a range of times. The UV–vis detection is converted to mass of drug released (b and d) using the established calibration curve. The errors represent the standard deviation about the mean ($p^* < 0.05$). The values in the bracket show the total charge injected during stimulation.

PPy.FOS film once stimulation is removed as is used in the cochlea ear implant stimulation protocol [24].

The amount of FOS release increased linearly as the duration of stimulation increased. The lowest amount of FOS release at 15 s stimulation at −120 μA was calculated to be 187 ng. The variations and trends observed in Fig. 8a and b were also observed in Fig. 8c and d for application of +120 μA. The lowest amount of FOS released at 15 s of +120 μA stimulation was approximately 270 ng. The data presented in Fig. 8 clearly indicates that decreasing the time of stimulation does not affect the latency but does decrease the time to return to baseline (i.e., cessation of FOS release) as well as reducing the amount of FOS released. The lowest amount of FOS released (approximately 35 ng) was observed when −40 μA was applied for 60 s (Fig. 7b), however under these stimulation conditions the latency time was the highest out of all of the stimulation conditions investigated. Presuming rapid effect, as seen in *in vitro* brain slice studies, it is expected that the delivery system developed here using detection/release latency of approximately 10–12 s will provide an efficacious clinical response.

4. Conclusions

An anti-epileptic drug was successfully incorporated into PPy with the release demonstrated to be linear with the duration of stimulation current applied. A low negative current was shown to release small amounts of FOS with long latencies while at higher current the latency is reduced, however larger amount of FOS are released. This highlights the need to combine the appropriate current stimulation magnitude with the stimulation duration in order to obtain the most appropriate dosage in the most suitable timeframe upon stimulation. The features of the seizure detection and drug delivery system developed in this work permit the tailoring of these parameters to meet individual patient needs, enabling personalized epilepsy treatment.

The system developed in this work demonstrates the potential of using ECoG recordings and stimulation hardware for seizure initiated drug release and drug dose control. This system, once miniaturized, and coupled with flexible ECoG recording electrodes will enable a new paradigm in seizure therapy. Conceivably such a strategy could be applied to therapy in other neurological conditions where a triggering signal could be identified, such as Parkinson's disease. The versatility of the system allows for precise control of stimulation parameters such that the quantity and duration of drug release can be modulated on-demand. These studies lay the platform for further development towards a fully integrated, autonomous, implantable system.

Acknowledgements

Funding from the Australian Research Council Centre of Excellence Scheme (Project Number CE 140100012) and the McKenzie Postdoctoral Fellowship are gratefully acknowledged. GGW is grateful to the ARC for support under the Australian Laureate Fellowship scheme (FL110100196). The authors also wish to acknowledge the design and fabrication facilities accessed through the Australian National Fabrication Facilities (ANFF) Materials Node. Dr Stephen Beirne and Dr Patricia Hayes are thanked for

their assistance in figure preparation, instrument set up and process optimization respectively.

References

[1] J.W. Sanders, The epidemiology of epilepsy revisited, Curr. Opin. Neuro. 16 (2003) 165–170.
[2] S.D. Shorvon, The epidemiology and treatment of chronic and refractory epilepsy, Epilepsia 37 (1996) S1–S3.
[3] K. Swarztrauber, S. Dewar, J. Engel Jr., Patient attitudes about treatments for intractable epilepsy, Epilepsy Behav. 4 (2003) 19–25.
[4] R.S. Fisher, A.L. Velasco, Electrical brain stimulation for epilepsy, Nat. Rev. Neurol. 10 (2014) 261–270.
[5] P. Kwan, M.R. Sperling, Refractory seizures: try additional antiepileptic drugs (after two have failed) or go directly to early surgery evaluation, Epilepsia 50 (2009) 57–62.
[6] S.M. Sisodiya, W.R. Lin, B.N. Harding, M.V. Squire, M. Thom, Drug resistance in epilepsy: expression of drug resistance proteins in common causes of refractory epilepsy, Brain 125 (2002) 22–31.
[7] D. Schmidt, W. Loscher, Drug resistance in epilepsy: putative neurobiologic and clinical mechanisms, Epilepsia 46 (6) (2005) 858–877.
[8] W. Loscher, Mechanisms of drug resistance, Epileptic Disord. 7 (2005) S3–9.
[9] A.J. Halliday, S.E. Moulton, G.G. Wallace, M.J. Cook, Novel methods of antiepileptic drug delivery – polymer-based implants, Adv. Drug Deliv. Rev. 64 (2012) 953–964.
[10] A.J. Halliday, T.E. Campbell, T.S. Nelson, K.J. McLean, G.G. Wallace, M.J. Cook, Levetiracetam-loaded biodegradable polymer implants in the tetanus toxin model of temporal lobe epilepsy in rats, J. Clin. Neurosci. 20 (2013) 148–152.
[11] A.J. Halliday, M.J. Cook, Polymer-based drug delivery devices for neurological disorders, CNS Neurol. Disord. Drug Targets 8 (2009) 205–221.
[12] M.T. Salam, M. Mirzaei, M.S. Ly, D.K. Nguyen, M. Sawan, An implantable closedloop asynchronous drug delivery system for the treatment of refractory epilepsy, IEEE Trans. Neural Sys. Rehab. Eng. 20 (2012) 432–442.
[13] E. Kharlampieva, V. Kozlovskaya, J. Tyutina, S.A. Sukhishvil, Hydrogen-bonded multilayers of thermoresponsive polymers, Macromolecules 38 (2005) 10523–10531.
[14] S. Koh, S.K. Han, Y.W. Choi, J.H. Lee, J.Y. Lee, S.H. Yuk, Hydrogen-bonded polymer gel and its application as a temperature-sensitive drug delivery system, Biomaterials 25 (2004) 2393–2398.
[15] T. Serizawa, D. Matsukuma, M. Akashi, Loading and release of charged dyes using ultrathin hydrogels, Langmuir 21 (2005) 7739–7742.
[16] D.T. Auguste, S.P. Armes, K.R. Brzezinska, D.T. Deming, J. Kohnand, R.K. Prudhomme, pH triggered release of protective poly(ethylene glycol)-b-polycation copolymers from liposomes, Biomaterials 27 (2006) 2599–2608.
[17] P.M. George, D.A. LaVan, J.A. Burdick, C.Y. Chen, E. Liang, R. Langer, Electrically controlled drug delivery from biotin-doped conductive polypyrrole, Adv. Mater. 18 (2006) 577–581.
[18] R. Wadhwa, C.F. Lagenaur, X.T. Cui, Electrochemically controlled release of dexamethasone from conducting polymer polypyrrole coated electrode, J. Control. Release 110 (2006) 531–541.
[19] C.L. Recksiedler, B.A. Deore, M.S. Freund, A novel layer-by-layer approach for the fabrication of conducting polymer/RNA multilayer films for controlled release, Langmuir 22 (2006) 2811–2815.
[20] Y. Lin, G.G. Wallace, Factors influencing electrochemical release of 2,6-anthraquinone disulphonic acid from polypyrrole, J. Control. Release 30 (1994) 137–142.
[21] B. Massoumi, A. Entezami, Controlled release of sulfosalicylic acid during electrochemical switching of conducting polymer bilayers, Eur. Polym. J. 37 (2001) 1015–1020.
[22] M.R. Abidian, D.H. Kim, D.C. Martin, Inside front cover: conducting-polymer nanotubes for controlled drug release, Adv. Mater. 18 (2006) 405–409.
[23] G.G. Wallace, G.M. Spinks, L.A.P. Kane Maguire, P.R. Teasdale, Conductive Electroactive Polymers: Intelligent Material Systems, 1st edn., CRC, Press, Boca Raton, 2003.
[24] B.C. Thompson, S.E. Moulton, J. Ding, R.T. Richardson, A. Cameron, S. O'Leary, G.G. Wallace, G.M. Clark, Optimizing the incorporation and release of a neurotrophic factor using conducting polypyrrole, J. Control. Release 11 (2006) 285–294.
[25] B.C. Thompson, S.E. Moulton, R.T. Richardson, G.G. Wallace, Effect of the anionic dopant on nerve growth and controlled release of a neurotrophic protein from polypyrrole, Biomaterials 32 (2011) 3822–3830.
[26] B.C. Thompson, J. Chen, S.E. Moulton, G.G. Wallace, Nanostructured substrates enhance the controlled release of a neurotrophic protein from polypyrrole, Nanoscale 2 (2010) 499–501.
[27] T.M. Higgins, S.E. Moulton, K.J. Gilmore, G.G. Wallace, M. in het Panhuis, Gellan gum doped polypyrrole neural prosthetic electrode coatings, Soft Mater. 7 (2011) 4690–4695.
[28] G.G. Wallace, G.M. Spinks, L.A.P. Kane-Maguire, P.R. Teasdale, Conductive Electroactive Polymers: Intelligent Material Systems, Second edn., CRC Press, Boca Raton, 2003 (and references cited therein).
[29] R. Estellar, J. Echauz, T. Tcheng, B. Litt, B. Pless, Line length: an efficient feature for seizure onset detection, Eng in Med. Biol. Soc., 2001. Proc. of the 23rd Annual Int. Conf. of the IEEE. 2 (2001) 1707–1710.
[30] R.T. Richardson, B.C. Thompson, S.E. Moulton, G.G. Wallace, R.M.I. Kapsa, G.M. Clark, S. O'Leary, Polypyrrole with incorporated NT3 promotes auditory nerve survival and neurite outgrowth, Biomaterials 28 (2007) 513–523.
[31] B. Rambeck, U.H. Jurgens, T.W. May, H.W. Pannek, F. Behne, A. Ebner, A. Gorji, H. Straub, E.J. Speckmann, B. Pohlmann-Eden, W. Loscher, Comparison of brain extracellular fluid, brain tissue, cerebrospinal fluid, and serum concentrations of antiepileptic drugs measured intraoperatively in patients with intractable epilepsy, Epilepsia 47 (4) (2006) 681–694.

Biographies

Rikky Muller is an Assistant Professor of Electrical Engineering and Computer Science (EECS) at UC Berkeley. She received her bachelor's and master's degrees at MIT and her Ph.D. degree at UC Berkeley in EECS. She was a McKenzie fellow and Lecturer of Electrical and Electronic Engineering at the University of Melbourne. Prof. Muller co-founded Cortera Neurotechnologies, a medical device company where she held positions as CEO and CTO. She is the winner of numerous awards and fellowships and was named one of 35 global innovators under the age of 35 (TR35) by the MIT Technology Review for her work in the field of technology and medicine.

Zhilian Yue is a senior research fellow at the institute of Intelligent Polymer Research Institute, the ARC Centre of Excellence for Electromaterials Science, University of Wollongong, Australia. She received her PhD from Heriot-Watt University, UK, in 2002. Her current research interests are in the area of functional polymers for controlled release of bioactive molecules and 3D bioprinting for tissue repair and regeneration.

Sara Ahmadi is a PhD student who is perusing her doctorate degree under the supervision of Profs Wallace, Moulton and Cook. Her studies involve investigating the use of conducting polymer structures to control the delivery of antiepilepsy drug.

Winston C.W. Ng is a graduate of The University Of Melbourne, Australia, having received his Masters of Engineering (Electrical) (Distinct) in 2014. Having particular skills and passion in signal processing and electronics design, Winston is currently working at Melbourne based company Tekt Industries, which provides engineering services in areas including embedded systems and IoT.

Willo Grosse graduated with a PhD from University of Wollongong in 2014 and has since moved to work in the finance sector with Ernst and Young as part of the Research & Development Team.

Mark Cook is a Professor of Medicine, University of Melbourne, and Director of Neurology, St. Vincent's Hospital Melbourne. His current interests are in polymer based drug delivery systems, imaging, brain modelling, and neurophysiology.

Gordon Wallace is Director of the ARC Centre of Excellence for Electromaterials science headquartered at the University of Wollongong. His research interests include the design and synthesis of new electromaterials and the development of additive fabrication protocols to enable assembly of novel structures and devices containing them-for use in energy and medical bionics.

Simon Moulton is Professor of Biomedical Electromaterials Science at Swinburne University of Technology. His field of research is developing organic conducting materials for use in a variety of applications ranging from sensors to biomedical application. He has a strong track record in materials chemistry research spanning electroactive materials as well as conventional biomaterials.